ISBN: 978-3-95450-247-9 ISSN: 2673-5490 doi: 10.18429/JACoW-IPAC2024-MOPR89

FRAMEWORK FOR A MULTIPHYSICS MODEL OF OPTICAL FIELD EMISSION FROM EXTENDED NANOSTRUCTURES*

J. I. Mann†, J. B. Rosenzweig, UCLA, Los Angeles, CA, USA

Abstract

Laser-field emission, or optical field emission, is a process that can produce electron beams with high charge density and high brightness with ultrafast response times. Using an extended nanostructure, such as a nanoblade, permits plasmonic field enhancement up to 80 V/nm with an incident ultrafast laser of wavelength 800 nm. Stronger ionizing fields lead to higher current densities, so understanding how this field is attained will aid in further increasing brightness. In this paper we lay the framework to study the nanoblade system thermomechanically and plasmonically. We show that, in the moving frame following the laser driver, a steady state is reached, allowing us to reduce the computational complexity of the multiphysics calculation. We derive Maxwell's equations and the current dynamical equation for the steady state in such a moving frame. We also derive the eigenproblem for finding plasmonic modes in the structure with a nonlinear dielectric. The planned calculations to come will allow us to predict peak attainable fields and optimal experimental parameters. We leave off with a discussion of directions for numerical implementation.

INTRODUCTION

Nanostructured cathodes such as nanotips are commonplace in various devices, including electron microscopes [1] and electron guns [2]. The benefit of using such cathodes is that the applied electric or laser field is geometrically or plasmonically enhanced at the apex, reducing the total emission area and increasing the emitted current density. The end result is a decreased emittance and increased beam brightness. Another nanostructure, the nanoblade [3, 4], promises a larger baseline brightness in part due to the lack of curvature in one axis [5]. Perhaps even more impactful is its ability to withstand strong fields – nanotips with ultrafast THz illumination have reached transient surface fields of 40 V/nm [6] while nanoblades have reached 80 V/nm [4] under similar conditions. In the image charge limited regime, this two-fold improvement in field strength brings about a four-fold increase in current density [3, 5].

The blade's higher field tolerance is attributed to its geometry: a blade uniformly illuminated along its apex has two degrees of freedom to disperse thermal energy, while a narrow tip has only one [7]. This finding's underlying analysis was rather simplistic, using a thermalized two-temperature model of solid gold structures and a simple surface heating model based on dielectric and vacuum heating losses. These limitations meant that the comparison between two structures may be accurate, but absolute results (e.g., peak temperatures and damage) must be more carefully interpreted. There are several aspects which must be improved upon, as discussed in the paper. Here we will focus on producing a holistic model including the temperatures (and any non-thermal components), the Maxwell fields, vacuum charge dynamics, nonlinearities, and temperature-dependent dielectrics. Further, the blade is not only one material; it is a metal-coated silicon wedge (see the diagram in Fig. 1a).

This is a computationally expensive prospect if we wish to solve the system fully in 3-D and through time, particularly considering that we will want to perform several calculations for varying laser intensities, incident angles, and structure properties. In this paper we first argue that the system reaches a steady state, allowing us to remove the time dependence and make the study more tractable. We then lay some of the framework necessary to solve for the Maxwell fields in the moving frame for which the steady state exists. We finally discuss the next steps for modeling and numerical implementation.

STEADY-STATE ARGUMENT

We treat the incident laser as a plane wave with infinite extent transversely and with a non-zero incident angle, as shown in Fig. 1b. Due to this incident angle, the phase front moves faster than the speed of light along the blade's edge. Additionally, in a frame which moves along the blade at this effective phase velocity, the free laser pulse is static.

We represent the state of the system as a state vector $u(\mathbf{r}, t)$, containing all relevant fields and space-time-dependent properties. The state at any point in space-time depends only on the solution in that point's past light cone, or domain of dependence (DOD), as stipulated by causality. We may write the state at $\mathbf{r}, t$ as a functional F of the state within the DOD of $\mathbf{r}, t$

$$u(\mathbf{r}, t) = F(\mathbf{r}, t)[u(\mathbf{r}', t')] \,, \tag{1}$$

such that F only operates on u within the DOD: $(\mathbf{r} - \mathbf{r}')^2 - c^2(t - t')^2 \leq 0$ and $(t - t') > 0$. This functional inverts the dynamical equation for the state vector and is itself invariant under space-time translations. The transformation to the moving frame (without Lorentz boosting) is

$$\xi = z - v_L t, \; t \to t \,, \tag{2}$$

with the laser's velocity along the blade $v_L = c \sec \phi \geq c$. Performing this transformation, the DOD is restricted to $\xi - \xi' = \Delta\xi \in [\Delta\xi_-, \Delta\xi_+]$ with

$$\Delta\xi_\pm = -v_L \Delta t \pm \sqrt{c^2 \Delta t^2 - \Delta\rho^2} \leq 0 \,, \tag{3}$$

* This research is supported by the Center for Bright Beams, U.S. National Science Foundation grant PHY-1549132.
† jomann@physics.ucla.edu

ISBN: 978-3-95450-247-9 ISSN: 2673-5490 doi: 10.18429/JACoW-IPAC2024-MOPR89

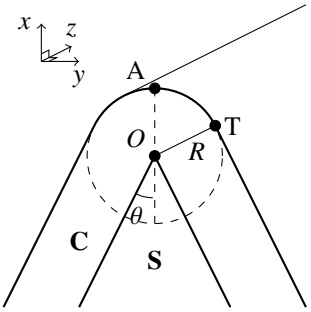

(a) Diagram of a nanoblade with half-opening angle θ and radius of curvature R. Labels include the apex A, the transition from curved to sloped at T, the apex of the substrate O, the substrate **S** and the coating **C**.

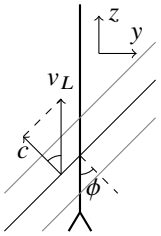

(b) Top-down view of the blade (vertical line) and the laser phase fronts (slanted lines). The laser has an incident angle ϕ (exaggerated here) leading to a phase velocity along the blade axis, z, of $v_L = c \sec\phi$.

Figure 1: Diagrams of the nanoblade and incident laser front.

with ρ the transverse (x-y) coordinate. Because both longitudinal bounds on $\Delta\xi$ are less than zero, the entire DOD lies ahead of $\mathbf{r}$. This can be seen in Fig. 2.

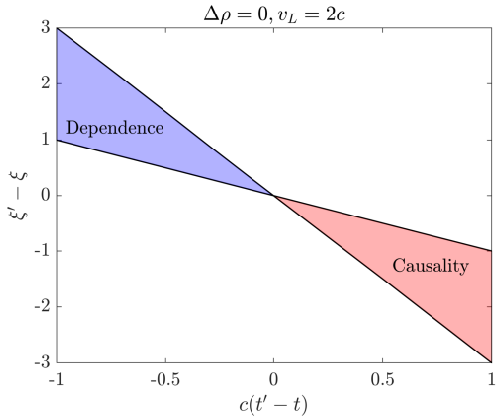

Figure 2: Domains of dependence (DOD) (i.e. past light cone) and causality for two points at the same transverse coordinate $\rho' = \rho$. The entire DOD for a particular point ξ lies ahead $\xi' > \xi$ and before $t' < t$ that point, effectively flushing any time-dependent component away. The laser phase front lies as a horizontal line on this plot, with vertical position depending on the relative position ξ.

Consider that the system does have an initial condition: the laser front reaching the beginning of the finite blade. As suggested, the material as a function of space-time is also part of the state vector. We then write this as the state being a combination of a piecewise constant externally applied state beginning at $z = 0$ and a general internal state

$$u(t) = \Theta(\xi + v_L t)u_{ext} + u_{int}(t) \ . \tag{4}$$

For the blade system this u_{ext} may be the material makeup of the blade's cross-section, and only existing for $z \geq 0$ as indicated by the Heaviside theta. There is then a perturbation at $\xi = -v_L t$ which leads to time-dependence within its domain of causality (future light cone). The forward-most point for which this perturbation is within the DOD is

$$\xi = -(v_L - c)t \ . \tag{5}$$

Thus, the unsteady part of the solution is "flushed" backwards at $v_L - c$ relative to the moving frame. For a total pulse width of T_{pulse} a steady state is reached within this width after

$$T_{steady} = T_{pulse}(1 - \cos\phi)^{-1} \ , \tag{6}$$

where we have also considered the increased length of the pulse along the z-axis with a factor of $\sec\phi$.

For instance, with an incident angle of 7 deg and a pulse width of $T_{pulse} = 8$ fs (akin to the experiment of Ref. [3]) a steady state within the pulse width is reached after $T_{steady} = 1.1$ ps, or a length traveled of about 0.3 mm. For reference, the blade has multi-mm extent. Further, we expect a steady state to be reached far sooner as the system is lossy, with linear surface plasmon polaritons (SPP) on a gold surface having a decay length of about 100 µm (with dielectric constants for gold at 800 nm from Ref. [8]). This aids in analyzing experiments with more shallow incident angles (e.g., 1 deg in Ref. [4]). The remaining caveat is that of the Rayleigh length z_R: Ref. [3] has $z_R \approx 20$ µm which is too short for either the causality-induced or loss-induced steady state. The goal is to fully illuminate the blade [4], so in future experiments this complication may vanish.

2-D MODAL EQUATIONS

Here we lay out the equations for the 2-D SPP modes. The goal is to further understand the dispersion and behavior of the underlying SPP enhancement when additional considerations such as temperature and nonlinearities are at play. We begin with Maxwell's wave equations and assume that we are finding a mode with frequency ω and wavenumber $k = \mathbf{k} \cdot \hat{z}$ (into the page in Fig. 1a):

$$\partial_t \to -i\omega, \ \partial_z u = iku, \ \partial_z \epsilon = 0 \ . \tag{7}$$

The wave equation for the longitudinal E_z and transverse $E_\perp$ electric fields are

ISBN: 978-3-95450-247-9 ISSN: 2673-5490 doi: 10.18429/JACoW-IPAC2024-MOPR89

$$\begin{aligned} \nabla \times \nabla \times E_\perp + ik\nabla E_z + k^2 E_\perp &= \frac{\omega^2}{c^2}\epsilon(|E|)E_\perp \\ ik\nabla \cdot E_\perp &= \frac{\omega^2}{c^2}\epsilon(|E|)E_z \, . \end{aligned} \tag{8}$$

The dielectric constant may be moved to the left side to reveal the eigenproblem for an eigenvalue $\frac{\omega^2}{c^2}$, with a given k. We may approximate the third-order optical Kerr effect with the modified field-dependent dielectric function [9]

$$\epsilon(|E|) \approx \epsilon^{(1)} + \frac{3}{4}\chi^{(3)}|E|^2 \, . \tag{9}$$

For gold, $\chi^{(3)} \approx (2.2\,\mathrm{V/nm})^{-2}$ [10], indicating a strong nonlinearity in the V/nm regime. The field magnitude and the temperature may be taken from a more whole 3-D calculation, delegating this as a tool for investigating the underlying system once these quantities are known.

3D STEADY-STATE MODEL

Here we lay out the foundations for a moving-frame steady-state calculation, with the aim of using the finite element method (FEM) for solving. Ultimately we hope to include the temperature (and/or some representation of the Boltzmann equation for non-thermal dynamics), vacuum charge dynamics (resulting from quasi-static Fowler-Nordheim tunneling), and materials with temperature and field dependent dielectrics. For now we focus on the Maxwell fields and lay out the linear calculation.

Maxwell's Equations

We will use the potential formulation of Maxwell's equations in the Lorentz gauge:

$$\begin{aligned} \partial_i^2 \mathbf{A} - c^2 \dot{\nabla}^2 \mathbf{A} &= -J \\ \partial_i^2 \phi - c^2 \dot{\nabla}^2 \phi &= -\rho \, , \end{aligned} \tag{10}$$

where the overdot signifies the untransformed coordinate. Now we perform the coordinate transformation of Equation 2, and with steady state assumed in the resulting frame we get

$$\dot{\nabla} \to \nabla, \; \partial_i \to -v_L \partial_\xi, \; \partial_t = 0 \, , \tag{11}$$

and the wave equation becomes

$$\begin{aligned} (v_L^2 \partial_\xi^2 - c^2 \nabla^2)\mathbf{A} &= -\mathbf{J} \\ (v_L^2 \partial_\xi^2 - c^2 \nabla^2)\phi &= -\rho \, , \end{aligned} \tag{12}$$

ξ is a time-like coordinate here as $v_L > c$. All material properties will be embedded in the source terms $\mathbf{J}$ and ρ.

Charge Dynamics

We, of course, have the continuity equation

$$\partial_i \rho = \dot{\nabla} \cdot \mathbf{J} \, , \tag{13}$$

which transforms to

$$v_L \partial_\xi \rho + \nabla \cdot \mathbf{J} = 0 \, . \tag{14}$$

Additionally, the current will be driven by some function

$$\partial_i \mathbf{J} = -v_L \partial_\xi \mathbf{J} = \mathbf{Q}(\mathbf{E}, \mathbf{B}, \rho, \mathbf{J}) \, , \tag{15}$$

where the electric and magnetic fields may be calculated in the moving frame

$$\begin{aligned} \mathbf{E} &= -\nabla\phi + v_L \partial_\xi \mathbf{A} \\ \mathbf{B} &= \nabla \times \mathbf{A} \, . \end{aligned} \tag{16}$$

The microscopic driver $\mathbf{Q}$ embodies the properties of the participating charges. In vacuum this would just be the term resulting from the Lorentz force, or a boundary term due to field emission at the surface. The first step in our case, however, is to find the behavior for a linear dielectric. Microscopically, and in the untransformed frame, the current should be

$$\partial_i \mathbf{J} = \mathbf{Q}_{\epsilon^{(1)}} = \frac{\sigma}{\omega}\mathbf{E} - \tau^{-1}\mathbf{J} \, , \tag{17}$$

with σ the conductivity and τ^{-1} the relaxation rate. After assuming $\mathbf{J} \propto \mathbf{E} \propto e^{i\mathbf{k}\cdot\dot{\mathbf{r}} - i\omega i}$ we find that

$$\mathbf{Q}_{\epsilon^{(1)}} = -(\epsilon_r - 1)^{-1}\mathbf{E} - \frac{\omega\epsilon_i}{\epsilon_r - 1}\mathbf{J} \, , \tag{18}$$

where ϵ_r and ϵ_i are the real and imaginary relative dielectric functions, respectively, and are chosen at the primary driving frequency. We also have the boundary condition $\hat{n}\cdot\mathbf{J}|_{surf} = 0$ binding the charge to the material. This is also where quasi-static field emission may be applied.

DISCUSSION

With an argument for the inevitable steady state and the equations laying the framework for such a calculation, the next step is numerical implementation for the linear dielectric. We intend to solve the system using the finite element method (FEM), either solving in 3-D or in 2-D by treating ξ as a time-like coordinate. We have yet to choose the elements we will use – continuous H^1 elements with the standard weak formulation seem natural for the potentials, but a discontinuous Galerkin approach may be more effective for this advection-type problem.

Subsequently we will add nonlinearity, thermodynamics, and a temperature-dependent dielectric constant. We hope this will ultimately produce realistic peak temperatures and survivability predictions which we may then use to find optimal experimental parameters for achieving a higher brightness or stronger high-harmonic generation yields as predicted by the field distribution. Lastly, we hope to include vacuum charge dynamics ensuing from quasi-static field emission.

ISBN: 978-3-95450-247-9 ISSN: 2673-5490 doi: 10.18429/JACoW-IPAC2024-MOPR89

REFERENCES

[1] R. Bormann, S. Strauch, S. Schäfer, and C. Ropers, "An ultrafast electron microscope gun driven by two-photon photoemission from a nanotip cathode", *J. Appl. Phys.*, vol. 118, no. 17, p. 173 105, 2015. doi:10.1063/1.4934681

[2] B. Schröder, M. Sivis, R. Bormann, S. Schäfer, and C. Ropers, "An ultrafast nanotip electron gun triggered by grating-coupled surface plasmons", *Appl. Phys. Lett.*, vol. 107, no. 23, p. 231 105, 2015. doi:10.1063/1.4937121

[3] T. Paschen *et al.*, "Ultrafast strong-field electron emission and collective effects at a one-dimensional nanostructure", *ACS Photonics*, vol. 10, no. 2, pp. 447–455, 2023. doi:10.1021/acsphotonics.2c01551

[4] G. Lawler, N. Majernik, J. Mann, N. Montanez, J. Rosenzweig, and V. Yu, "Emittance Measurements of Nanoblade-Enhanced High Field Cathode", in *Proc. IPAC'22*, Bangkok, Thailand, June 2022, 2022, pp. 709–712. doi:10.18429/JACoW-IPAC2022-MOPOMS033

[5] J. Mann *et al.*, "Simulations of Nanoblade Cathode Emissions with Image Charge Trapping for Yield and Brightness Analyses", in *Proc. NAPAC'22*, Albuquerque, NM, USA, 2022, pp. 535–538. doi:10.18429/JACoW-NAPAC2022-TUPA86

[6] D. Matte *et al.*, "Extreme lightwave electron field emission from a nanotip", *Phys. Rev. Res.*, vol. 3, no. 1, p. 013 137, 2021. doi:10.1103/PhysRevResearch.3.013137

[7] J. Mann and J. Rosenzweig, "A Thermodynamic Comparison of Nanotip and Nanoblade Geometries for Ultrafast Laser Field Emission via the Finite Element Method", *Physics*, vol. 6, no. 1, pp. 1–12, 2024, Number: 1 Publisher: Multidisciplinary Digital Publishing Institute. doi:10.3390/physics6010001

[8] M. Magnozzi, M. Ferrera, L. Mattera, M. Canepa, and F. Bisio, "Plasmonics of au nanoparticles in a hot thermodynamic bath", *Nanoscale*, vol. 11, 2018. doi:10.1039/C8NR09038F

[9] G. New, *Introduction to Nonlinear Optics*. Cambridge University Press, 2011.

[10] J. Renger, R. Quidant, N. van Hulst, and L. Novotny, "Surface-enhanced nonlinear four-wave mixing", *Phys. Rev. Lett.*, vol. 104, no. 4, p. 046 803, 2010. doi:10.1103/PhysRevLett.104.046803